

DECAY HEAT REMOVAL UNDER BOILING CONDITION  
IN A PIN-BUNDLE GEOMETRY

August, 1980

Power Reactor and Nuclear Fuel Development Corporation

複製又はこの資料の入手については、下記にお問い合わせ下さい。

〒311-13 茨城県東茨城郡大洗町成田町4002

動力炉・核燃料開発事業団 大洗工学センター

システム開発推進部 技術管理室

Inquiries about copyright and reproduction should be addressed to:  
Technology Management Section, O-arai Engineering Center, Power Reactor  
and Nuclear Fuel Development Corporation 4002, Narita O-arai-machi Higashi-  
Ibaraki-gun, Ibaraki, 311-14, Japan

動力炉・核燃料開発事業団 (Power Reactor and Nuclear Fuel Development  
Corporation)

Paper presented to the 9th Liquid Metal Boiling Working Group Meeting

June 4-6, 1980  
Rome, Italy

DECAY HEAT REMOVAL UNDER BOILING CONDITION IN A PIN-BUNDLE GEOMETRY

K. Haga\*, M. Uotani\*, K. Yamaguchi\* and M. Hori\*

\* O-arai Engineering Center, Power Reactor  
and Nuclear Fuel Development Corporation, Japan ,

ABSTRACT

Decay heat removal capability under boiling condition was investigated using an electrically heated 37-pin bundle test section. The flow was driven by natural circulation force of the out-of-pile sodium loop SIENA in O-arai Engineering Center, PNC. As the heater power was increased, the two-phase flow regime changed from bubbly flow to slug flow and then to annular or annular mist flow. In 15 runs, dry-out was not observed in the average exit quality region of less than 0.5. The results indicated the existence of a large "boiling window" for low flow rate and low power conditions.

INTRODUCTION

In the analysis of Loss of Pipe Integrity (LOPI) and Loss of Shutdown Heat Removal System (LSHRS) accidents in a LMFBR, the reactor power is assumed to be less than 10 % of its normal operating condition. In the events where the core flow rate is degraded, sodium boiling can result. From the point of reactor safety, it is important to check the capability of heat removal by sodium boiling, because if permanent dry-out occurs, fuel pin melting will follow.

Some experiments have been made to investigate the dry-out phenomena under low flow rate conditions. Garrison et al.<sup>(1)</sup> conducted a series of natural convection sodium boiling experiments using a single-channel mockup heated by a radiant furnace. In their experiments, stable boiling was observed for a coolant power densities between 160 and 200 W/cm<sup>3</sup>, and film dry-out appeared between 200 and 210 W/cm<sup>3</sup>. These results were similar to those estimated by Hinkle<sup>(2)</sup> from his single-channel low pressure water boiling experiments under natural convection.

It is well known that, under transient conditions, voiding dynamics in a multi-channel bundle is different from that in a single-channel test section, because two-dimensional effects tend to ameliorate the course of the transient by delaying the onset of flow reversal and dry-out<sup>(3),(4)</sup>. To investigate the two-dimensional effects under decay heat level sodium boiling, experiments in bundle geometries were conducted by Kaiser et al.<sup>(5),(6)</sup>. In their seven-pin bundle test section, dry-out appeared when the inlet valve was

completely closed at the heat flux of  $8.3 \text{ W/cm}^2$ (5). In their 37-pin bundle test section, permanent dry-out was observed at the heat flux of  $11.7 \text{ W/cm}^2$  (linear heat rate of  $22 \text{ W/cm}$ ) and the estimated local quality of 0.8(6). The complete inlet valve closure represents an unrealistically severe condition being considered in the present study. Furthermore, the 37-pin bundle experiments were conducted without heating the central 6 pins because of a blockage plate attached to the central subchannels.

The present report deals with a series of out-of-pile experiments which were conducted with an electrically heated 37-pin bundle test section. The sodium flow was driven by natural circulation and boiling was accomplished by increasing heater power. After stable boiling was established, the heat input was further increased stepwise. Three runs were terminated by the occurrence of dry-out.

#### TEST FACILITY

The experiments were carried out in the Sodium Boiling and Fuel Failure Propagation Test Loop SIENA in O-arai Engineering Center, PNC. Figure 1 shows a schematic of the SIENA loop. The sodium from the test section flowed into the expansion tank, separator, cooler, pump and returned to the test section.

The test section is shown in Figure 2. The bundle consisted of 37 electrically heated pins. Tantalum was used as the heating element in the pins. The electrical resistance of tantalum is sensitively changed by the temperature such that the maximum heat flux under boiling condition was higher than the mean axial heat flux by 10 to 20 %. Each pin of 6.5 mm diameter was wrapped by a 1.3 mm diameter spacer wire with a 264.8 mm helical pitch. The diameters and the pin pitch of 7.9 mm were the same configuration with those in the MONJU fuel subassemblies. The bundle had a 450 mm heated length and a 750 mm simulated FP gas plenum at its downstream position. The 37 pins were installed in a hexagonal inconel tube of 10 mm thickness so that the gap between the peripheral pins and the inner duct wall was 1.45 mm. Thermal insulator on the outer wall of the hexagonal tube minimized heat losses through duct wall.

Chromel-Alumel thermocouples of 0.3 mm diameters were located at 10 cross-sections to measure pin surface and subchannel temperatures. They were embedded in the outer surface of pin sheath, and the probes for subchannel temperature measurement were projected from the pin surface. Subchannel thermocouples were also located in several spacer wires. The test section inlet and outlet temperatures and hexagonal tube temperatures were monitored by additional thermocouples. Two types of void-meter were used to detect voids. A total of 14 resistive void-meters were attached within the test section. In addition, a total of 10 Chen-type void-meters located in the spacer wires were used to detect local voids. The sodium velocities at the inlet and outlet of the test section were measured by electromagnetic flow-meters. Pressure transducers (Kaman type KP-1911, frequency response range: 0 to 8300 Hz) were also provided at the inlet and outlet of the test section to measure the pressure changes during boiling experiments.

#### OPERATING PROCEDURES AND TEST CONDITIONS

Prior to the boiling experiments, the linearity of inlet flow-meter was

checked in the low velocity range of 0.05 to 0.2 m/sec. The result showed acceptable accuracy (within  $\pm 7\%$ ) for the purpose of the present experiment.

The amount of the natural circulation sodium flow was controlled by an opening of inlet valve in the main loop. The oxygen concentration was kept under 10 ppm by the purification unit. After cover gas pressure, inlet temperature and valve openings were set, the heater power was increased stepwise until boiling was initiated. After stable boiling was observed, as indicated by temperature, void, flow rate and pressure signals, the heater power was increased further to higher levels. Argon gas was injected from the inlet tube of the test section in two runs (quality range of 0.014 to 0.017) to investigate the effect of noncondensable gas on the boiling phenomena.

One heater pin was failed in the early stage of test program and two additional pins were failed in the final stage. The majority of the runs were conducted using residual 36 heater pins.

The experimental conditions are summarized as follows:

Sodium system pressure	1.21 - 1.48 bar
Inlet temperature	324 - 486 °C
Flow velocity at boiling inception	0.03 - 0.18 m/sec
Heat flux (maximum)	6.9 - 51.4 W/cm <sup>2</sup>

#### TEST RESULTS

Figures 3-1 and 3-2 show pin surface temperatures (those measured at 6 different axial locations are gathered in Fig. 3-1 and those measured at 6 different radial locations near the end of heated section are in Fig. 3-2), inlet pressure and inlet flow-meter signals during the dry-out test (Run No. 37LHF-123).

When the thermocouples located at G-section (11.3 mm upstream from the end of heated section) showed the onset of boiling, the reading of inlet velocity was 0.18 m/sec and that of maximum heat flux was 42.2 W/cm<sup>2</sup>. After the onset of boiling, sodium flow was accelerated gradually due to natural circulation to yield the termination of boiling. The boiling duration time of this step was about 30 sec.

Then, the heat flux was raised to 45.5 W/cm<sup>2</sup> level and the continuous boiling was observed in the central subchannels of G-section and F-section (33.4 mm upstream from the end of heated section). The signal of void-meter C-07 indicated that the flow regime was bubbly flow.

When the heat flux was raised further more to 52.0 W/cm<sup>2</sup> level, oscillatory boiling appeared. It was proved by the succeeding power increases that the amplitude and period of inlet flow oscillation were increased with heat flux. At the heat flux of 56.6 W/cm<sup>2</sup>, as can be seen in Fig. 3-2, saturation temperature region near the end of heated section was extended radially toward the peripheral pins and duct wall. During this step, formation and collapse of vapor slugs caused the violent oscillations of inlet flow and pin surface temperatures measured at the outer subchannels. The pressure pulses measured at the inlet of the test section (P-108) corresponded to the collapses of large vapor slugs.

At the heat flux of 62.4 W/cm<sup>2</sup>, the two-phase region expanded upstream and reached B-section (257.4 mm upstream from the end of heated section). The oscillation of inlet flow was stabilized at a constant value of 0.09 m/sec. Figure 4 compares the signals of two types void-meters: the resistive void-meter VOT-\*\* and the Chen-type one C-\*\*. The void-meters VOT-9 and C-8 were located at the same axial position. At the latter half of this experimental

step, the void-meter signals became to take certain plateau levels, i.e. the conditions of almost whole cross-section being filled by sodium vapor. Therefore, it was considered that the flow regime was altered from slug to annular or annular mist flow.

After the heat flux was raised to  $63.4 \text{ W/cm}^2$  the signal measured by the thermocouple T-204G showed a steep increase due to the occurrence of dry-out, and the pin power was cut by the pin protection limit ( $1000 \text{ }^\circ\text{C}$ ) switch. During this run, inlet sodium temperature was maintained at  $370 \text{ }^\circ\text{C}$ .

Figure 5 shows the typical signals of temperature, pressure and inlet flow in the next dry-out test (Run No. 37LHF-124). This run was conducted under the conditions of three pins being unheated and flow resistance in the main circulation loop being increased by the further closing of the inlet valve. The inlet sodium temperature was  $372 \text{ }^\circ\text{C}$ .

Boiling was detected at the heat flux of  $11.0 \text{ W/cm}^2$  and the inlet velocity of  $0.05 \text{ m/sec}$ . In such a low flow condition, radial temperature profile becomes almost flat except the immediate vicinity of duct wall. This profile caused almost simultaneous boiling initiation within the whole cross-section at the end of heated section.

After the occurrence of regular flow oscillation, it was decayed to a constant value. This tendency between heat flux and inlet flow rate was similar to that observed in the previous run. The saturation temperature region reached B-section at the heat flux of  $29.9 \text{ W/cm}^2$ . Although the signal measured by the thermocouple T-204G showed a temporary dry-out, the peak temperature was not high enough to terminate the test.

At the further increase of heat flux to  $42.8 \text{ W/cm}^2$  level, the inlet flow velocity attained a new level of  $0.05 \text{ m/sec}$  and the heater power was cut by detecting the temperature overshoot of the thermocouple T-204G.

Figure 6 shows resistive void-meter signal during this run. Liquid slugs were no longer detected at the heat flux range of greater than  $29.9 \text{ W/cm}^2$  as was the case in the previous run.

Figure 7 shows the map of heat flux versus initial single-phase flow velocity. Dry-outs were measured in three of the 15 runs conducted. Within the tested conditions, noncondensable gas did not affect the dry-out heat flux.

## DISCUSSIONS

As is seen from the signals of flow-meters and void-meters, the flow pattern was changed with heat flux from bubbly flow to slug flow and then to annular or annular mist flow. The change of two-phase flow pattern was essentially the same with that observed in the forced circulation experiment with single-pin test section<sup>(7)</sup>. It was in the annular or annular mist flow regime that dry-out appeared. It is natural for us to consider that the dry-out in this flow regime is caused by the disappearance of liquid film on the pin surface under high quality conditions.

From the heat balance of the test section, the average exit quality at the end of the heated section was calculated from heat flux and flow velocity tested. In this calculation, the time averaged inlet flow velocity was used in the steps where the inlet flow velocity showed oscillations.

Figure 8 shows a comparison between the average exit qualities estimated for every step of the present dry-out tests with the dry-out qualities derived in the 19-pin bundle tests of ORNL. The horizontal line means the local dry-out quality derived in the 37-pin bundle tests of KfK. Except high velocity

region ( $> 0.4$  m/sec), the dry-out quality in every case was more than 0.5.

Many empirical equations of the critical conditions beyond which the dryout will appear have been proposed for water two-phase flow. In these equations, mass flow rate, heat flux, quality, pressure etc. are included as the effective parameters. However, few equations cover the low pressure and low flow rate conditions. Biasi et al.<sup>(8)</sup> obtained the equation using their experimental results. The covered experimental conditions (mass flow rate: 100 to 6000 Kg/m<sup>2</sup>sec, pressure: 2.7 to 140 Kg/cm<sup>2</sup> and pipe inner diameter: 3 to 3.75 mm) were relatively close to those of the present sodium experiments. The calculated dry-out quality from their equation is 0.95 for one of the present cases. Except the verification of the applicability of their equation to the sodium flow conditions, one of the major causes of the difference between calculated value and the actual data of the present sodium experiments may lie in the non-uniform radial distribution of local qualities in the tested pin bundle.

These results shows the existance of a large "boiling window" under low power condition. This conclusion is also expected to stand in a reactor subassembly (unless the inlet flow of a subassembly is completely stopped). Consequently, the decay heat may be removed by sodium boiling when the small amount of inlet flow rate is assured by natural circulation.

#### CONCLUSIONS

Experimental study was carried out to investigate natural circulation boiling in a 37-pin electrically heated LMFBR fuel subassembly mockup. The observed flow regime changed from bubbly flow to slug flow and then to annular or annular mist flow in the average exit quality range of less than 0.5. The result indicated the existance of a large "boiling window" at low power conditions in a pin-bundle geometry.

Further study will be required to identify the decay heat dry-out criteria and natural circulation.

#### ACKNOWLEDGMENTS

The authors wish to acknowledge the technical contributions of Mr. T. Isozaki, Mr. T. Komaba and Mr. K. Sahashi at all stages of the present experiments.

#### REFERENCES

1. P. W. Garrison et al., International Meeting on Fast Reactor Safety Technology, Seattle, 1686-1695 (1979)
2. W. D. Hinkle, HNL-Sub-4450-1 (MIT-EL 76-005) (1976)
3. Y. Kikuchi et al., J. Nucl. Sci. Technol., 15-2, 100-108 (1978)
4. J. L. Wantland et al., International Meeting on Fast Reactor Safety Technology, Seattle, 1678-1685 (1976)
5. A. Kaiser et al., CONF 761005-517-7 (1976)
6. A. Kaiser et al., ENS/ANS Topical Meeting on Nuclear Power Reactor Safety, Brussel (1978)
7. Y. Kikuchi et al., J. Nucl. Sci. Technol., 12-2, 83-91 (1975)
8. L. Biasi et al., Energia Nuclear 14, 9 (1967)

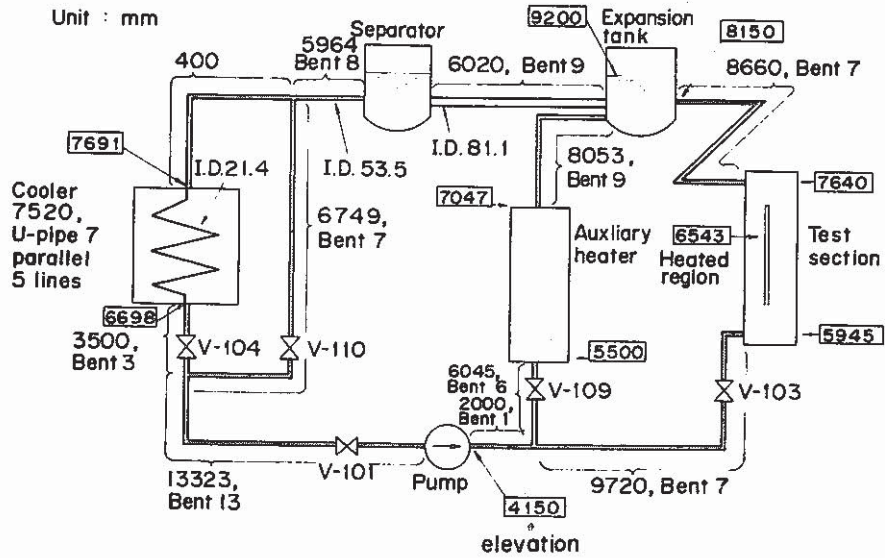


Fig. 1 Geometries of main line and elevations from floor

(PNC-FS-960)

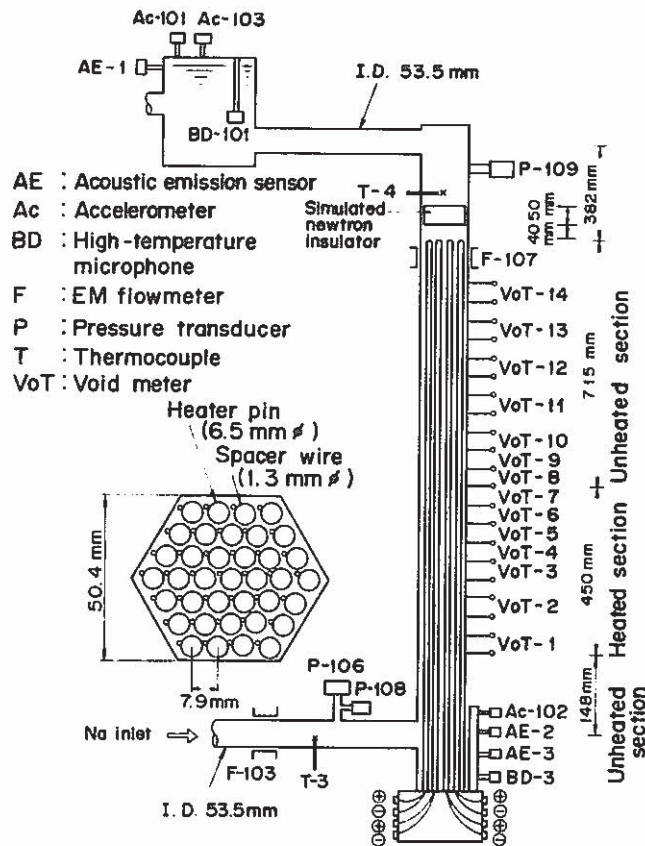


Fig. 2 Wire-wrapped 37-pin bundle test section, 37F T.S.

(PNC-FS-962)



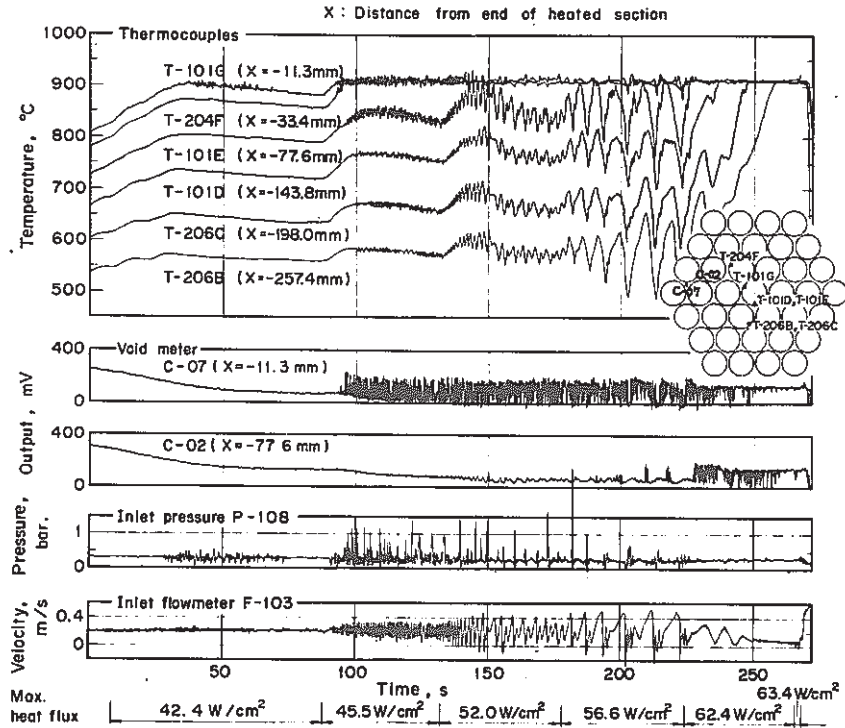


Fig. 3-1 Signals of sodium temperatures, inlet and outlet flow velocities during the dry-out test, Run No. 37LHF-123 (PNC-FS-1112)

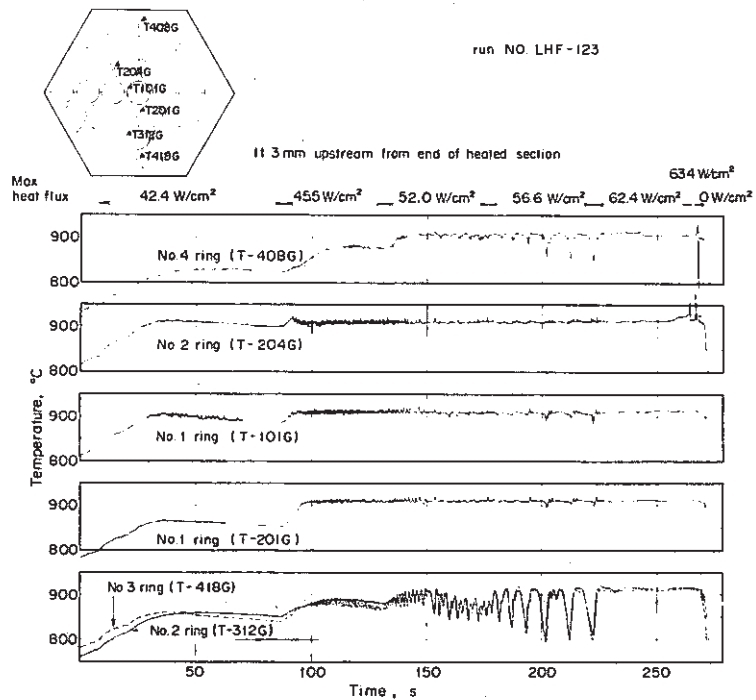


Fig. 3-2 Signals of pin surface temperatures measured at G-section during the dry-out test, Run No. 37LHF-123 (PNC-FS-978)

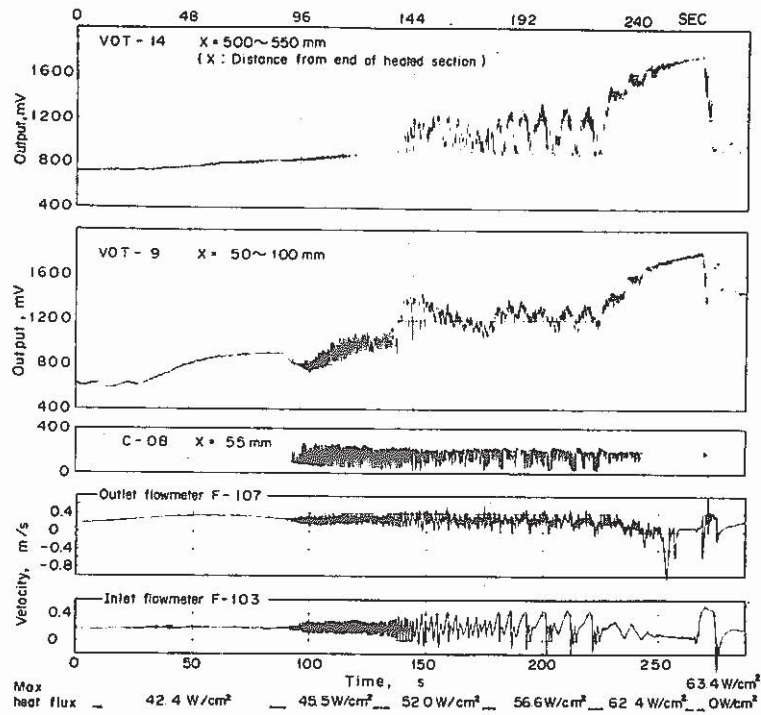


Fig. 4 Signals of two types void-meters: the resistive void-meter VOT-\*\* and the Chen-type void-meter C-\*\*, during the dry-out test, Run No. 37LHF-123 (PNC-FS-977)

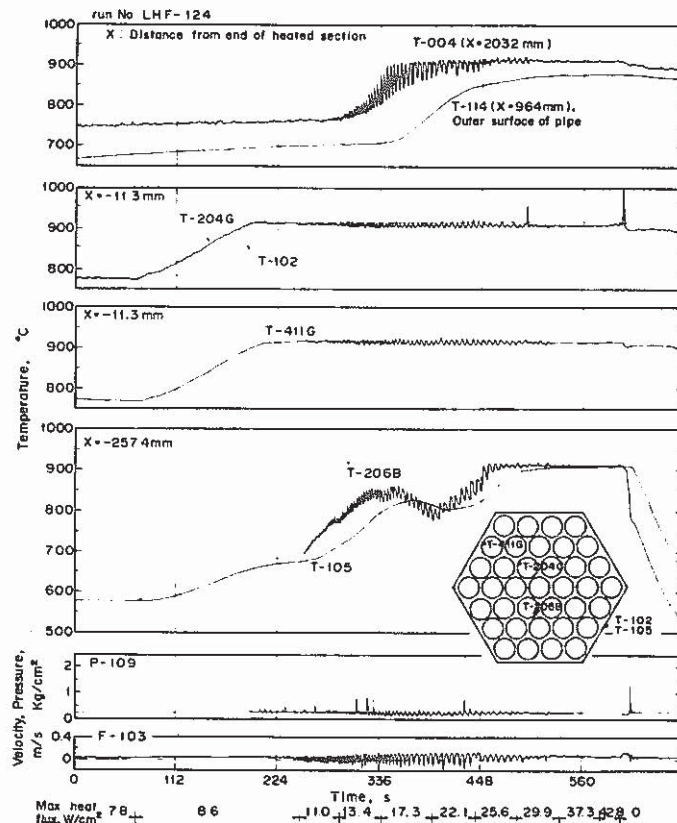


Fig. 5 Signals of temperatures, pressure and inlet flow velocity during the dry-out test, Run No. 37LHF-124 (PNC-FS-989)

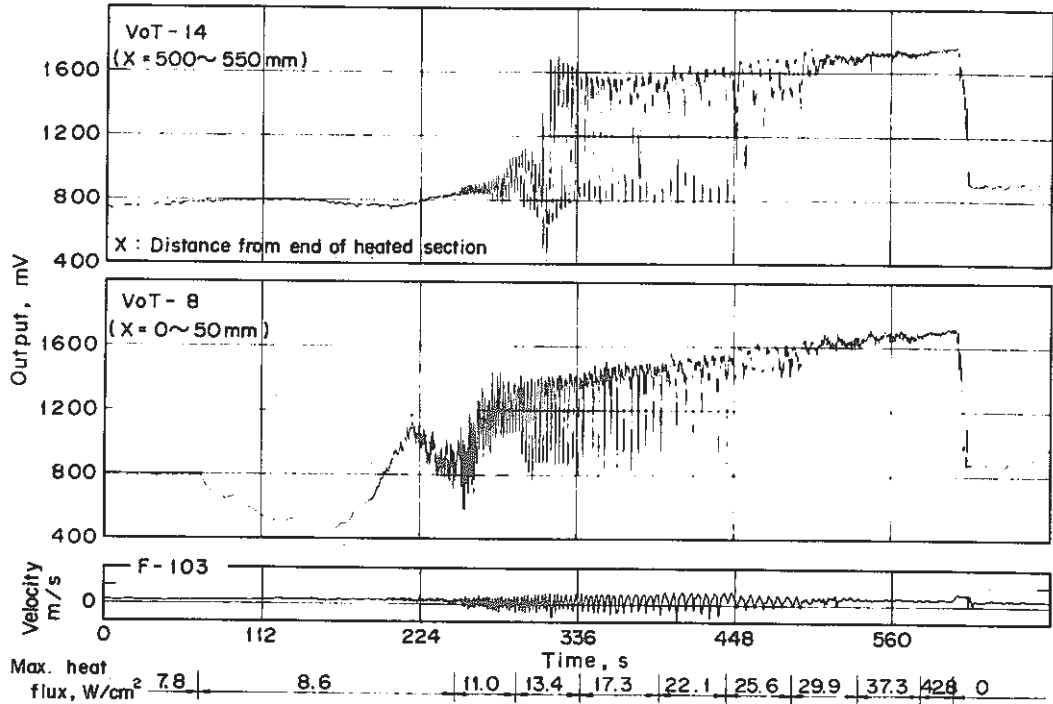


Fig. 6 Signals of resistive void-meters and inlet flow velocity during the dry-out test, Run No. 37LHF-124 (PNC-FS-990)

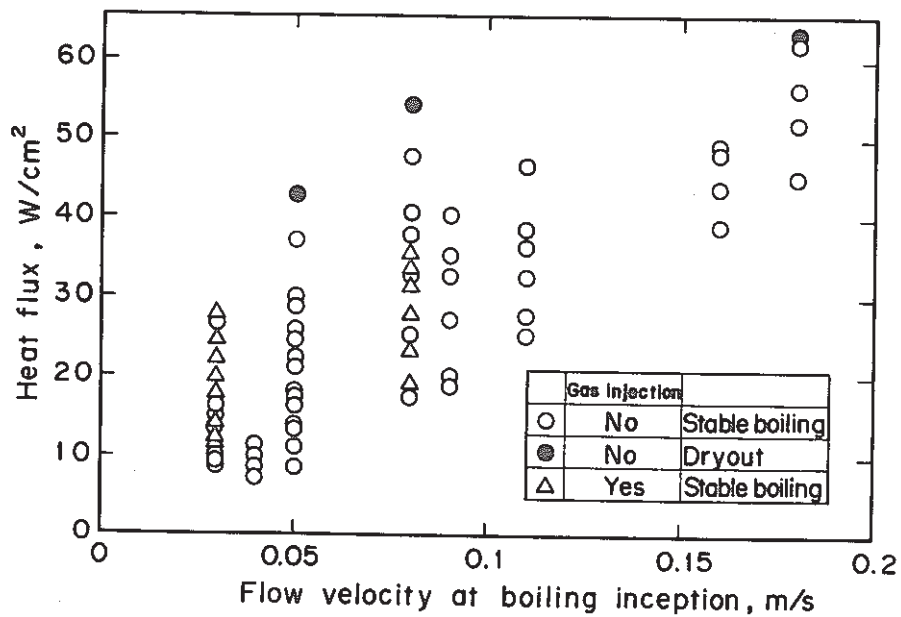


Fig. 7 Experimental conditions of heat fluxes versus initial value of inlet flow velocities (PNC-FS-992)

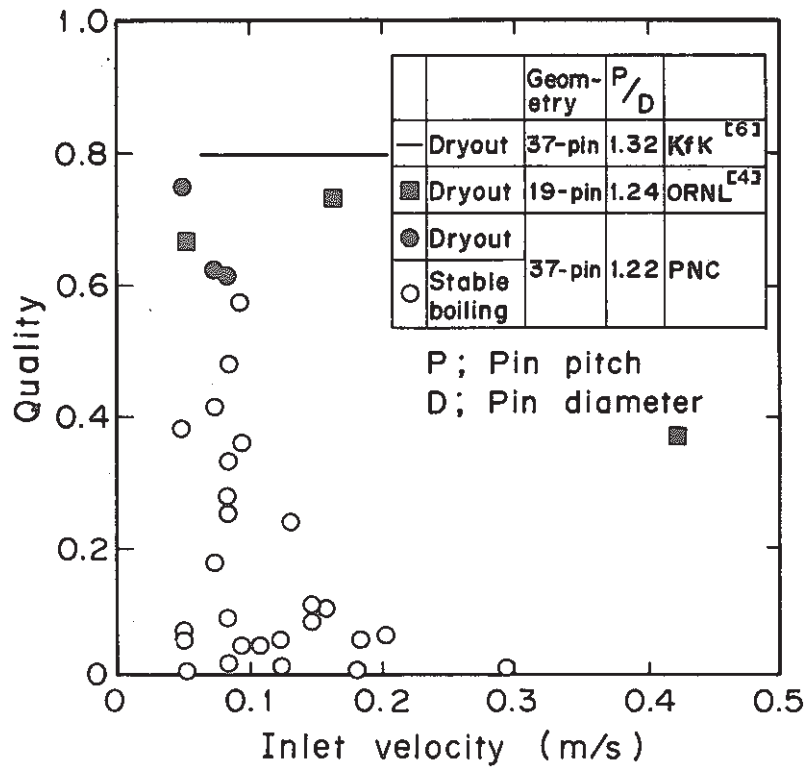


Fig. 8 Comparison between the qualities of the present dry-out tests with available data of dry-out qualities in pin bundles (PNC-FS-1113)